Robust Integrated Sensing and Communications in Delay-Doppler Domain Using Superimposed Training

Méndez-Monsanto Suárez, Lianet; Chen Hu, Kun; Fernández-Getino García, Maria Julia; García Armada, Ana

Published in:
2023 IEEE Globecom Workshops (GC Wkshps)

DOI (link to publication from Publisher):
10.1109/GCWkshps58843.2023.10464932

Publication date:
2023

Document Version
Accepted author manuscript, peer reviewed version

Robust Integrated Sensing and Communications in Delay-Doppler Domain using Superimposed Training

Lianet Méndez-Monsanto Suárez[1], Kun Chen-Hu[1,2], María Julia Fernández-Getino García[1], Ana García Armada[1]
[1]Department of Signal Theory and Communications, Universidad Carlos III de Madrid, Spain
[2]Department of Electronic Systems, Aalborg University, Denmark
E-mails: {lianet, kchen, mjulia, agarcia}@tsc.uc3m.es

***Abstract*—Emerging Sixth Generation (6G) communication network promises to operate in non-trivial high-mobility conditions and the integration of sensing capabilities, such as in vehicle-to-vehicle communications, high-speed trains and satellites. Orthogonal time-frequency space (OTFS) is an appealing waveform capable of transmitting data to the users and, at the same time, estimate the range and speed of the targets thanks to the delay-Doppler domain. However, OTFS also suffers from a large pilot overhead in channel estimation procedure. In this paper, a novel joint sensing technique and data transmission is proposed based on superimposed training (ST), which is capable of nullifying the overhead while maintaining an affordable computational complexity and overall performance.**

***Index Terms*—ISAC, OTFS, channel estimation, superimposed-training**

I. Introduction

The forthcoming Sixth Generation (6G) communications network [1] will deliver new services in many challenging scenarios. Among these applications, the joint use of intelligent target sensing and broadband communications, known as Integrated Sensing and Communications (ISAC), will have a major impact on the industry. It is expected to reshape future landscapes by offering a range of possibilities, from precise positioning and smart urban infrastructure to wearable Internet of Things (IoT) devices. Moreover, this combination of capabilities holds great promise for high-mobility scenarios such as autonomous vehicles, satellites, and drones, as it is not only capable of establishing reliable communications, but also efficiently providing real-time information of the devices by using the existing resources dedicated to communications [2].

Orthogonal time-frequency space (OTFS) [3]–[5] is one of the most appealing broadband waveforms for high-mobility scenarios. Because it multiplexes data symbols in the delay-Doppler (DD) domain, it is able to remove the time-varying effect of Doppler spread, unlike orthogonal frequency-division multiplexing (OFDM). Recently, OTFS has also been exploited for sensing [5], since the range and velocity of the targets of interest can be easily obtained from sufficiently accurate channel estimates in the DD domain. However, OTFS suffers from a high pilot overhead when realistic channel estimation and equalization procedures are considered. According to [3], [6], a set of guard symbols (zeros) must surround each pilot in order to avoid the self-interference produced by the data symbols, and thus a relevant data rate degradation is produced.

Channel estimation based on superimposed training (ST) with OTFS, i.e. ST-OTFS, has been recently proposed in the literature to avoid this overhead problem [4], [5]. In ST-OTFS, both data and pilot symbols are superimposed and transmitted in the same resource in the DD domain, which produce a zero overhead system. However, a self-interference induced by the data symbols in the superposition process must be considered at the receiver. Current ST-OTFS channel estimation procedures are not able to filter out the self-interference induced by the data symbols before providing the equalizers: [4] performs the channel estimation by using minimum mean squared error (MMSE) criterion, in which the self-interference is considered as an additional source of interference/noise in the computation of covariance matrices, and hence, both channel estimates and the sensing parameters (range and velocity) are only accurate in very high signal to noise ratio (SNR) cases. Later, [5] performs a successive interference cancellation approach for both channel estimation and data detection. At each iteration, these procedures are refined at the expense of increasing the complexity of the receiver, which also increases the latency of the system.

The main aim of this work is to provide a joint sensing and data transmission scheme that is able to filter out the self-interference caused by using the ST approach in OTFS systems. Exploiting the properties of zero-mean data and noise, we propose an averaging method in the DD domain capable of reducing the self-interference generated by the ST technique, unlike the state-of-the-art solutions [4], [5], which rely on computationally intensive iterative interference cancellation schemes that do not fully address the interference. By properly filtering out this interference, our technique enhances the robustness of channel estimation and sensing against both interference and noise, thereby enabling improved performance in low signal-to-noise ratio (SNR) scenarios. We describe the channel estimation and sensing method and propose an appropriate pilot pattern design in the DD domain to enable the effective averaging technique, which, to the best of the authors' knowledge, has not been proposed before.

In our technique, the Doppler shifts and delays of each path of the channel are first estimated by performing block averaging in the Doppler domain followed by a bank of correlators. Then, the accurate channel gains are obtained by using a low-complexity interference cancellation method. The proposed techniques require less number of complex products while providing better estimates due to the fact that the noise and self-interference terms are effectively filtered out. Some simulation results will verify our analytical expressions and validate our proposal.

The remainder of the paper is organized as follows. Section II presents the OTFS system model. Section III introduces the proposed pilot design. Section IV explains the proposed ST-OTFS method. It details the procedure for obtaining the estimated sensing and communications parameters. Section V presents an analysis of the computational complexity of the proposed method and the comparison with the existing references. In Section VI, we present the simulation results. Finally, in Section VII, the conclusions are reported.

Notation: in this work, matrices, vectors and scalar quantities are represented by boldface uppercase, boldface lowercase, and normal letters, respectively. $[\mathbf{A}]_{m,n}$ denotes the element in the m-th row and n-th column of $\mathbf{A}$. $[\mathbf{a}]_n$ is the n-th element of the vector $\mathbf{a}$. $[\mathbf{a}]^{(n)}$ is the resulting vector from right-shifting n samples of vector $\mathbf{a}$. $\mathbf{I}_M$ is the identity matrix of size $(M \times M)$. $\mathbf{A} = \text{diag}\,(\mathbf{a})$ is a diagonal matrix whose diagonal elements are formed by the elements of vector $\mathbf{a}$. The superscripts $(\cdot)^T$ and $(\cdot)^H$ denote transpose and hermitian operations, respectively. $\otimes$ is the Kronecker product. $\odot$ denotes the Hadamard product. $\mathbb{E}\{\cdot\}$ represents the expected value. $\mathcal{CN}(0, \sigma^2)$ is the circularly-symmetric and zero-mean complex normal distribution with variance σ^2. $U(a, b)$ is the uniform random distribution between a and b. $\mathbb{C}^K$ and $\mathbb{Z}^K$ are K-dimensional complex and integer spaces, respectively, and $\mathbb{C}^{K\times K}$ is the $K \times K$-dimensional complex space. vec$(\mathbf{A})$ is the vectorized form of matrix $\mathbf{A}$. circ$[\cdot]$ is the circulant matrix.

II. System Model

According to the OTFS signaling [3]–[5], the zero padding-OTFS (ZP-OTFS) is exploited, which consists on appending a ZP of length L_{ZP} samples to the end of each multi-carrier symbol to absorb the intersymbol interference (ISI). At the transmitter, the complex data and pilot symbols are mapped in a resource grid that belongs to the DD domain. Then, an inverse discrete Zak transform (IDZT) is used to transform these symbols into samples that belong to the delay-time domain. The signal is propagated through a frequency and time selective channel, whose expression in the DD domain is given by

$$h(\tau, \nu) = \sum_{i=1}^{L_p} g_i e^{-j2\pi\nu_i\tau_i}\delta(\tau - \tau_i)\delta(\nu - \nu_i) \tag{1}$$

where L_p is the number of propagation paths and g_i are the channel gains. τ_i and ν_i are the delay and Doppler shifts, respectively, which can be expressed as

$$\tau_i = \frac{l_i}{M\Delta f} \leq \tau_{max} = \frac{l_{max}}{M\Delta f}, \tag{2}$$

$$\nu_i = \frac{k_i}{NT} \quad |\nu_i| \leq \nu_{max} \tag{3}$$

where M corresponds to the number of samples per each multi-carrier symbol and it also represents the number of delay bins, while N corresponds to the number of multi-carrier symbols to be transmitted, and it is also the number of Doppler bins. $l_i, k_i \in \mathbb{Z}$ are the integer normalized delay and Doppler shifts, respectively. By assuming that the channel is underspread [3]–[5] ($\tau_{max}\nu_{max} \ll 1$ and $T\Delta f = 1$), the normalized delay and Doppler shifts are constrained to $l_{max} < M$ and $-N/2 \leq k_i < N/2$.

Finally, the received signal is transformed back to the DD domain by using the discrete Zak transform (DZT) [7], [8].

Following [3]–[5], the received symbols $\mathbf{y} \in \mathbb{C}^{MN}$ of an OTFS signal can be modeled by making use of the equivalent channel in the DD domain as

$$\mathbf{y} = \mathbf{H}\mathbf{x} + \mathbf{z}, \tag{4}$$

where $\mathbf{x} \in \mathbb{C}^{MN}$ is the transmitted data symbol vector that belongs to a quadrature amplitude modulation (QAM) constellation, whose energy of the signal is normalized to one ($\mathbb{E}\left\{\left|[\mathbf{x}]_i\right|^2\right\} = 1,\ 1 \leq i \leq MN$). $\mathbf{z} \in \mathbb{C}^{MN}$ represents the additive white Gaussian noise (AWGN) whose distribution is given by $\mathcal{CN}\left(0, \sigma_z^2\right)$, and $\mathbf{H} \in \mathbb{C}^{MN\times MN}$ denotes the equivalent channel matrix in the DD domain, which is modeled as [4], [6], [9]

$$\mathbf{H} = (\mathbf{F}_N \otimes \mathbf{I}_M)\left(\sum_{i=1}^{L_p} g_i e^{-j2\pi\nu_i\tau_i}\mathbf{\Pi}^{l_i}\mathbf{\Delta}^{k_i}\right)(\mathbf{F}_N^H \otimes \mathbf{I}_M). \tag{5}$$

where $\mathbf{F}_N \in \mathbb{C}^{N\times N}$ denotes the normalized Fourier transform (DFT) matrix, $\mathbf{\Pi} \in \mathbb{C}^{MN\times MN}$ is the forward cyclic-shift (permutation) matrix and $\mathbf{\Delta} = \text{diag}\left(\left[1, e^{j2\pi\frac{1}{MN}}, ..., e^{j2\pi\frac{MN-1}{MN}}\right]\right)$.

III. Design of the Superimposed Pilot Sequence in the DD Domain

Let us define a pilot sequence $\mathbf{p} \in \mathbb{C}^M$ as

$$\mathbf{p} = [p_0, ..., p_{M-1}]^T = [e^{j2\pi\phi_{p_0}}, ..., e^{j2\pi\phi_{p_{M-1}}}]^T \tag{6}$$

where ϕ_{p_b} is the phase of the pilot and $b = 0, 1, ..., M - 1$. Then, the pilot sequence is repeated for each multi-carrier symbol as

$$\mathbf{x}_p = \mathbf{1}_{(N\times 1)} \otimes \mathbf{p} \in \mathbb{C}^{MN}. \tag{7}$$

This is visually represented in Fig. 1. This pilot design makes it possible to perform an averaging method in the DD domain, so that the interference and the noise can be reduced by a factor of N. Since the receiver design will be based on correlations, it will be helpful if these sequences have good autocorrelation properties. In this work, the pilots have unit magnitude and the phases are randomly generated with uniform distribution $U(0, 2\pi)$.

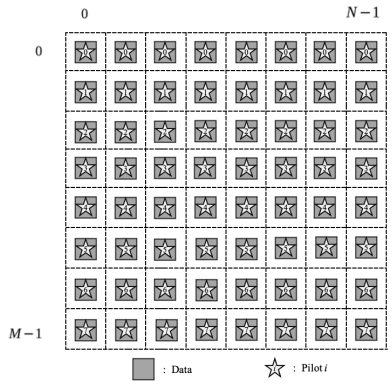

Fig. 1. Proposed pilot design in the DD domain for $M = 8$ and $N = 8$.

IV. Channel Estimation and Sensing Based on ST

This section details the proposed technique for obtaining the estimated delay and Doppler shifts $\tilde{l}_i, \tilde{k}_i$, respectively, and the estimated channel complex gains $\tilde{g}_i$, which allows to know the estimated channel matrix $\tilde{\mathbf{H}}$ in the DD domain. With this, it is possible to find out the estimated range and relative velocity of the detected targets and also to compensate the channel effects to recover the transmitted data symbols.

At the transmitter, the data symbols and the pilot sequence are superimposed as

$$\mathbf{x} = \sqrt{\beta}\mathbf{x}_d + \sqrt{1-\beta}\mathbf{x}_p, \tag{8}$$

where β represents the power assigned to the data. The received signal from (4) can be rewritten as

$$\mathbf{y} = \mathbf{H}\mathbf{x}_d + \mathbf{H}\mathbf{x}_p + \mathbf{z} \in \mathbb{C}^{MN}, \tag{9}$$

A. Pre-processing: Averaging in the DD domain

With an averaging technique of the received signal, the data and the Gaussian noise cancel out, leaving only the pilots and the channel, so that the latter can be estimated. This will be the main idea of our proposal.

The received signal in the DD domain, i.e. $\mathbf{y}$, can be repositioned in a matrix form $\mathbf{Y} \in \mathbb{C}^{M\times N}$, where $\mathbf{y} = \text{vec}(\mathbf{Y}) = \mathbf{H}\ \text{vec}(\mathbf{X})$. The first step of the proposed technique will be to perform an averaging along the rows of $\mathbf{Y}$, in other words, over N. This is equivalent to multiplying the received signal $\mathbf{y}$ by an averaging matrix $\mathbf{W}$ of size $M \times MN$, which is defined as follows

$$\overline{\mathbf{y}} = \frac{1}{N}\mathbf{W}\mathbf{y} = \frac{1}{N}\left(\mathbf{1}_{(1\times M)} \otimes \mathbf{I}_N\right)\mathbf{y}, \tag{10}$$

where $\overline{\mathbf{y}} \in \mathbb{C}^M$ is the averaged received vector $\mathbf{y}$. Making use of the fact that the data and noise samples are zero-mean random variables [4] ($\mathbb{E}\{\mathbf{x}_d\} = \mathbb{E}\{\mathbf{z}\} = 0$), the averaging will be capable of reducing the self-interference produced by the data symbols and the noise effects. Hence, (10) can be expressed as

$$[\overline{\mathbf{y}}]_m = \sum_{i=1}^{m}\sum_{n=1}^{L_{p,(l_i)}} g_n p_{m-i+1} e^{j2\pi\frac{k_n(m-i-l_n)}{MN}} + x'_d + z', \tag{11}$$

where $L_{p,(l_i)}$ denotes the number of propagation paths with delay l_i, where $i = 1, ..., m$, with m being the position of the vector $\overline{\mathbf{y}}$. The terms x'_d and z' denote the residual data self-interference and the residual noise effects, respectively, with variance

$$\sigma^2_{x'} = \frac{\beta}{N}, \quad \sigma^2_{z'} = \frac{\sigma^2_z}{N}, \tag{12}$$

where $\sigma^2_{x'}$ denotes the variance of the residual self-interference from the data and $\sigma^2_{z'}$ is the variance of the residual noise effects after the averaging over N. This means that averaging reduces both variances by a factor of N.

B. Estimation of the Delay and Doppler Shifts

Since the possible values of the normalized Doppler shifts will be bounded by $-N/2 \le k_i < N/2$, we propose to use a bank of correlators to obtain the estimate of the normalized delay and Doppler shifts of the received signal. We define the reference vector of Doppler exponentials $\boldsymbol{\kappa}_{k_i}$ as

$$\boldsymbol{\kappa}_{k_i} = e^{j2\pi\frac{k_i q}{MN}} \in \mathbb{C}^{MN} \text{ with } q = 0, ..., MN-1, \tag{13}$$

$$\frac{1}{MN}\boldsymbol{\kappa}_{k_i}\boldsymbol{\kappa}^H_{k_j} = \begin{cases} 1, & \text{if } i = j, \\ 0, & \text{otherwise.} \end{cases} \tag{14}$$

where it is satisfied that different Doppler reference vectors are orthogonal to each other. Therefore, the main idea is based on cross-correlating the averaged received vector $\bar{\mathbf{y}}$ with the reference Doppler vectors multiplied by the pilots, i.e.

$$\boldsymbol{\kappa}_{k,p} = \boldsymbol{\kappa}_k(M) \odot \mathbf{p} = \left[p_0 e^{j2\pi\frac{0}{MN}}, ..., p_{M-1}e^{j2\pi\frac{k_i(M-1)}{MN}}\right]^T, \tag{15}$$

so that correlation peaks will be obtained when the Doppler vector is present in the received signal. The term (M) in $\boldsymbol{\kappa}_k(M)$ refers to the first M samples of the vector. Then, (11) can be expressed as a function of $\boldsymbol{\kappa}_{k,p}$ as

$$[\overline{\mathbf{y}}]_m = \sum_{i=1}^{m}\sum_{n=1}^{L_{p,(l_i)}} g_n \left[\boldsymbol{\kappa}_{k_n,p}\right]_{m-i+1} + x'_d + z', \tag{16}$$

which means that the averaged received signal $\overline{\mathbf{y}}$ is the linear combination of different shifted versions of $\boldsymbol{\kappa}_{k,p}$. Since the shift of $\boldsymbol{\kappa}_{k,p}$ is given by the tap delay, using the scalar product we can obtain both the estimated delay and Doppler shift.

We define a matrix $\mathbf{C}^{(\text{abs})} \in \mathbb{R}^{N\times M}$, which stores the values of the cross-correlations between $\boldsymbol{\kappa}_{k,p}$ and $\bar{\mathbf{y}}$, this is

$$[\mathbf{C}^{(\text{abs})}]_{k,l} = \frac{1}{M}\left|\overline{\mathbf{y}}[\boldsymbol{\kappa}^H_{k,p}]^{(l)}\right| \tag{17}$$

with $l = 0, ..., M-1$. In other words, each row of the matrix stores the correlation between $\overline{\mathbf{y}}$ and shifted copies of the Doppler reference vector $\boldsymbol{\kappa}_{k,p}$. Therefore, the estimates of the normalized delay and Doppler shifts will be given by

$$(\tilde{k}_i, \tilde{l}_i) = \arg\max_{k,l}\left[\mathbf{C}^{(\text{abs})}\right]_{k,l}. \tag{18}$$

In order to ensure that the estimated delay and Doppler shifts are the correct ones, an additional check is performed as

$$[\mathbf{C}^{(\text{abs})}]_{k,l} \underset{\tilde{l}_i\neq l, \tilde{k}_i\neq k}{\overset{\tilde{l}_i=l, \tilde{k}_i=k}{\gtrless}} \gamma \tag{19}$$

where γ is a decision threshold, which is typically chosen according to the signal-to-interference-plus-noise ratio (SINR) of the system. The selection of this threshold is further discussed in our work in [10].

C. Estimation of the Channel Complex Gains

After estimating the normalized delay and Doppler shifts $\tilde{l}_i$ and $\tilde{k}_i$, we propose a low-complex iterative process to calculate the channel complex gains $\tilde{g}_i$. Given that, at this point, $\tilde{l}_i$ and $\tilde{k}_i$ are known, we have $\tilde{L}_p$ as the number of estimated propagation paths and we know the evolution of the Doppler exponentials and the taps delays (i.e. positions) along the vector $\bar{\mathbf{y}}$. This means that the only unknowns left to find out in the vector are the complex gains of the channel g_i.

The procedure follows two steps:

a) Forward step: Thanks to the staggered structure of the averaged received vector $\bar{\mathbf{y}}$, a coarse estimation of the complex gains $\tilde{g}_i^{(0)}$ can be obtained traversing the vector $\bar{\mathbf{y}}$ forward or *downstairs*, i.e. $i_d = 1, ..., L_p - 1$, using the first position of each tap. To start, the coarse channel gain for the first tap, i.e., $\tilde{g}_1^{(0)}$ can be given by dividing the first position of the vector $\bar{\mathbf{y}}$ by the first position of the reference Doppler exponential with pilots $\boldsymbol{\kappa}_{\tilde{k},p}$, of the the first estimated tap (i.e. $\tilde{k} = \tilde{k}_1$). The general expression is

$$\tilde{g}_{i_d}^{(0)} = \frac{\left[\bar{\mathbf{y}}_{i_d}\right]_{1+l_{i_d}}}{\left[\boldsymbol{\kappa}_{\tilde{k}_{i_d},p}\right]_1} = \left[\bar{\mathbf{y}}_{i_d}\right]_{1+l_{i_d}} e^{-j2\pi\phi_{p_0}} e^{-\phi_{\kappa_0}}, \tag{20}$$

where $\boldsymbol{\phi}_\kappa = [\phi_{\kappa_0}, ..., \phi_{\kappa_{M-1}}] = \arg\{\boldsymbol{\kappa}_k(M)\}$. Note that the division in (20) is equivalent to a phase rotation, since the magnitude of $\boldsymbol{\kappa}_{k,p}$ and $\mathbf{p}$ is unitary. Later, the first tap can be removed from the vector as

$$\bar{\mathbf{y}}_{i_d+1} = \bar{\mathbf{y}}_{i_d} - \tilde{g}_{i_d}^{(0)} \boldsymbol{\kappa}_{k,p}(M - l_{i_d}). \tag{21}$$

With (20) and (21), we obtain all the coarse estimations of the channel complex gains for the first $\tilde{L}_p - 1$ paths. These estimates are said to be coarse because the vector $\bar{\mathbf{y}}$ has only been averaged by N, and therefore will present residual self-interference induced by the data. This is why the next step will be necessary.

b) Backward step: For $i_u = \tilde{L}_p$, the vector $\bar{\mathbf{y}}_{i_u}$ has only one tap left to be estimated. Instead of (20), this time the fine estimation of the channel gain $\tilde{g}_{i_u}$ is obtained using the complete $\bar{\mathbf{y}}$ and $\boldsymbol{\kappa}_{k,p}$ vectors and averaging by $M - l_{i_u}$, as

$$\begin{aligned}\tilde{g}_{i_u} &= \mathbb{E}\left\{\bar{\mathbf{y}}_{i_u} / \boldsymbol{\kappa}_{\tilde{k}_{i_u},p}(M - l_{i_u})\right\} \\ &= \frac{1}{M - l_{i_u}} \sum_{n=0}^{M-l_{i_u}} \frac{[\bar{\mathbf{y}}_{i_u}]_n}{[\boldsymbol{\kappa}_{\tilde{k}_{i_u},p}(M - l_{i_u})]_n} \\ &= \frac{1}{M - l_{i_u}} \sum_{n=0}^{M-l_{i_u}} [\bar{\mathbf{y}}_{i_u}]_n e^{-j2\pi\phi_{pn}} e^{-\phi_{\kappa n}}\end{aligned} \tag{22}$$

where '/' denotes the component-wise division. This average significantly reduces the data self-interference (as well as the AWGN) and provides a finer estimation of the complex channel gains. After this, the variances further reduce in a factor of M, i.e. $\sigma_{x''}^2 \propto \beta/MN$ and $\sigma_{z''}^2 \propto \sigma_z^2/MN$. Evaluating (22) for $i_u = \tilde{L}_p$ gives the fine estimate of the last tap $\tilde{g}_{\tilde{L}_p}$. Then, the vector $\bar{\mathbf{y}}$ must be traversed backwards or *upstairs*, i.e. $i_u = \tilde{L}_p, ..., 1$, to obtain the rest of fine estimates. This is, removing the estimated paths up to i_u,

$$\bar{\mathbf{y}}_{i_u+1} = \bar{\mathbf{y}}_{i_u} - \sum_{n=1}^{\tilde{L}_p - i_u + 1} \tilde{g}_n \boldsymbol{\kappa}_{k_n,p}(M - l_n). \tag{23}$$

D. Data detection and sensing

Once the delay and Doppler shifts and the complex channel gains are known, the estimated channel matrix $\tilde{\mathbf{H}}$ can be obtained and the MMSE equalization method is employed to obtain the estimated data vector

$$\hat{\mathbf{x}}_{\text{MMSE}} = \left(\tilde{\mathbf{H}}^{\text{H}}\tilde{\mathbf{H}} + \sigma_z^2 \mathbf{I}_{MN}\right)^{-1} \tilde{\mathbf{H}}^{\text{H}}\mathbf{y}. \tag{24}$$

The delay and Doppler shifts have a direct relationship with the range and relative velocity of the targets, i.e. $r \propto \tau c$ and $v \propto \nu c/f_c$ where c is the speed of light and f_c is the carrier frequency.

Passive sensing is considered in this work. That is, the communications receiver acts as a sensing receiver, i.e., it estimates the parameters related to the distance and relative velocity of the targets from the received communications signal. Typical ISAC scenarios of this case appear in [5] and [11], where it is possible to sense a target that reflects a non-line of sight (NLoS) tap with a LoS tap as a reference. In this paper, for further generalization, we present the results in terms of the estimation capability of the normalized delay and Doppler shifts.

V. Computational Complexity Analysis

In this section, we evaluate the computational complexity of the proposed ST-OTFS technique in terms of the number of complex products. Table I shows the comparison of the proposed method and the existing ST-OTFS techniques in [4], [5] and the embedded-pilot (EP) technique, i.e. non-ST approach in [6], also visually represented in Fig. 2.

In the existing method in [4], S is the constellation size and N_I refers to the number of iterations of the message passing (MP) algorithm. In the technique in [5], the number of iterations N_I refers in this case to the iterative channel estimation

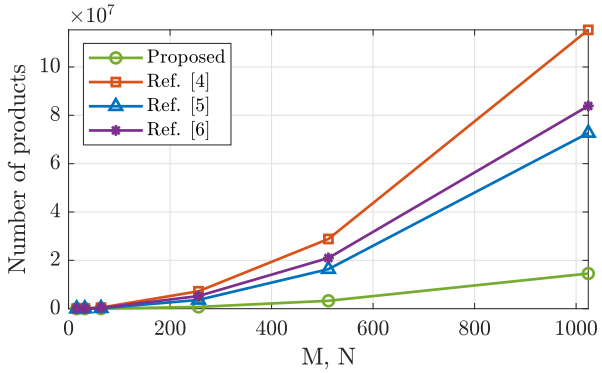

Fig. 2. Complexity comparison in number of products between the proposed and the existing ST-I [4], ST for DFT-s-OTFS [5] and the existing EP [6].

TABLE I
COMPLEXITY COMPARISON

Proposed	
Operation	**# Products**
Complex gain calculator	$(L_p-1)(M-l_i+1)$
Channel MMSE Equalizer	$\propto MN\log(MN)$
Existing ST-NI, ST-I (per iteration) [4]	
Operation	**# Products**
MMSE estimate of channel (Step 1)	$L_p^2MN+L_p^2+L_p$
MMSE estimate of channel (Step 2)	$\propto L_p^3$
MMSE estimate of channel (Step 3)	$L_p(MN+1)$
MMSE estimate of channel (Step 4)	L_p^2
Data detection using MP	$\propto N_I MNL_pS$
Existing ST for DFT-s-OTFS [5]	
Operation	**# Products**
Two-phase estimation algorithm	$\propto MN\log(MN)$
Iterative channel estimation and data detection	$\propto N_I MN\log(MN)$
Existing EP [6]	
Operation	**# Products**
Step 1	$(2k_{max}+1)(l_{max}+1)$
Step 2	$5L_p$
Data detection using MP	$\propto N_I L_pS(MN-(2l_{max}+1)(4k_{max}+1))$

and data detection technique, which usually converges within 2 to 5 iterations. It can be seen that the proposed method in this work reduces the computational cost, where the term $O(MN\log(MN))$ corresponds to the channel matrix inversion, which is performed only once.

In fact, for the proposed technique, the bank of correlators implies a number of products of M^2N. However, this can be avoided since these operations can be performed in the phase domain, since both the Doppler exponent and the pilots have unit magnitude in (17). This converts the complex products to additions, further reducing complexity. In this case, only the conversion of the complex numbers from binomial to polar form needs to be considered. In practice, this could be simply implemented using CORDIC algorithms [12].

The dominant term in the complexity of the proposed method is the inversion of the matrix $\tilde{\mathbf{H}}$ of size $MN\times MN$. In a general case, the inversion of this matrix would be of the order of $O(MN^3)$. However, when considering integer delay and Doppler shifts, the matrix is block-circulant and the complexity is reduced to only $O(MN\log(MN))$. Moreover, by using ZP-OTFS, this matrix has the highest sparsity among all OTFS variants.

VI. RESULTS

In this section, we present the results in terms of bit error rate (BER), mean squared error (MSE) of the channel estimate, the velocity and the range. The simulation parameters are:

- $M=512$, $N=16$.
- Carrier frequency $f_c=26$ GHz.
- Subcarrier spacing of $\Delta f=60$ kHz.
- Modulation of QPSK.
- The complex channel gains follow a random Rayleigh distribution. The delay and Doppler shifts are random integers with $l_{max}<M$ and $-N/2\le k_i<N/2$.

The root mean squared error (RMSE) expression for the normalized delay $s=l$ and Doppler $s=k$ shifts is

$$E_s=\left|\frac{1}{\tilde{L}_p}\sum_{i=1}^{\tilde{L}_p}|\tilde{s}_i|-\frac{1}{L_p}\sum_{i=1}^{L_p}|s_i|\right| \quad \text{for } s=l,k. \tag{25}$$

The MSE for the channel estimate is

$$E_H=\mathrm{Tr}\left[(\mathbf{H}-\tilde{\mathbf{H}})(\mathbf{H}-\tilde{\mathbf{H}})^H\right]. \tag{26}$$

Fig. 3 and Fig. 4 show the estimation accuracy in terms of the RMSE (E_l and E_k) for the normalized delay l_i and Doppler k_i shifts, respectively, in the case of one target $L_p=1$. We use one target in order to compare the proposed method to the scenario of passive sensing in [5]. In [5], they perform a coarse two-phase estimation algorithm to obtain g_i, k_i and l_i, and later do an iterative MMSE channel estimation and data detection. They use a single pilot, to which they assign higher power, acting as a flag. Although their iterative technique allows them to reduce interference, they do not eliminate it completely. For this reason, our results are more robust in low SNR scenarios. The bank of correlators is able to accurately detect the target, thanks to its ability to filter out the interference and noise.

Fig. 5 shows the comparison of the proposed method and the references for the channel MSE (E_H), in the case of $L_p=5$ propagation paths. The results for both references [5] and [4] are the theoretical expressions for MSE provided by the authors, this means that, in practice, the results will be

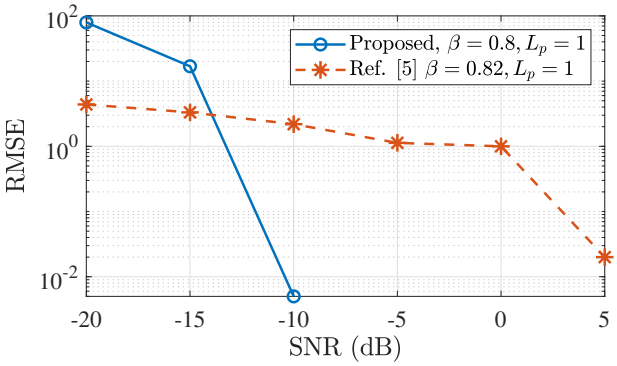

Fig. 3. RMSE of the normalized delay shift (E_l). $L_p=1$.

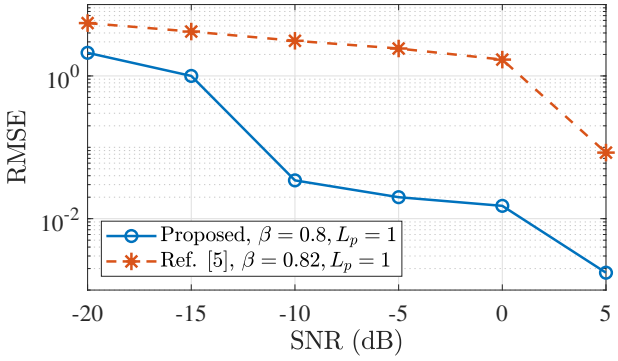

Fig. 4. RMSE of the normalized Doppler shift (E_k). $L_p=1$.

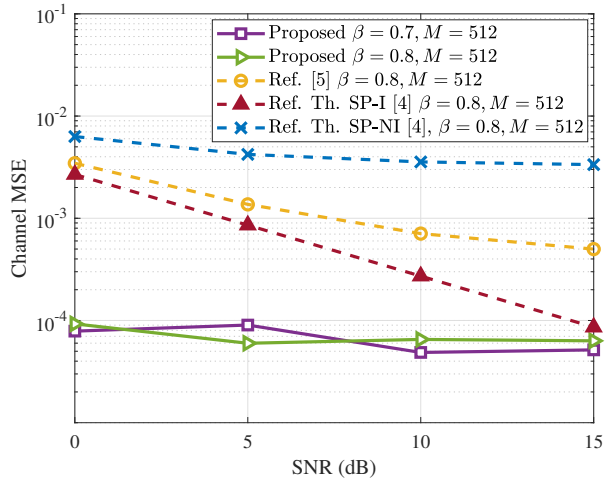

Fig. 5. Channel MSE (E_H) for the proposed method and references [4] and [5]. $L_p = 5$.

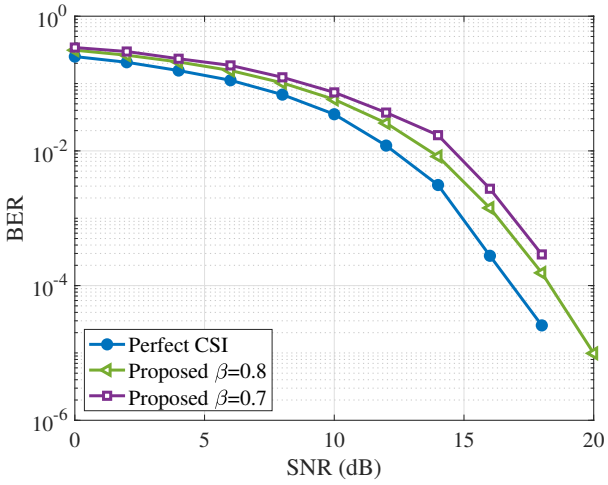

Fig. 6. BER vs. SNR comparison for the proposed method. $L_p = 2$.

greater than or equal to the curve shown. For [4], we show the existing channel MSE results for their superimposed non-iterative (ST-NI) and iterative (ST-I) methods. It is observed that the proposed technique outperforms the references. In the proposed method, the self-induced data interference and the noise effects are successfully filtered out by averaging, and the improvement in performance with respect to the references is significant, specially in low-SNR scenarios, obtaining a MSE reduction of approximately one order of magnitude. However, the effectiveness of the averaging depends on having a sufficient number of samples of the received signal. That is, the MSE of the channel is reduced as the value of M and N increases.

Fig. 6 shows the BER for the perfect channel state information (CSI) case (as a reference of performance), and the results for the proposed method for $\beta = 0.8$ and $\beta = 0.7$. The number of propagation taps in this case is of $L_p = 2$. The power assigned to the data is a trade-off between estimation accuracy and detection performance. With a very high value of β, the data are given a higher power, and thus higher robustness to interference and noise during detection, but at the expense of sacrificing channel estimation accuracy.

VII. Conclusions

In this work, we propose a ST technique in an OTFS system that allows filtering the data interference using an averaging technique in the DD domain, unlike the existing works so far, which either are not able to filter this interference before providing the equalizer or use complex iterative techniques for its cancellation. We propose the appropriate pilot sequence for this and show the estimation process of the channel and sensing parameters for its use in ISAC. The proposed technique requires a smaller number of complex products and, at the same time, produces better estimates because the noise and self-interference terms are effectively filtered out. The results show that the technique is robust and can be applied in particular to environments with a low SNR.

Acknowledgments

This work has been supported by the Spanish National project IRENE-EARTH (PID2020-115323RB-C33/AEI /10.13039/501100011033). The authors would like to acknowledge the conversations with partners of the INTERACT COST action CA20120. The work of K. Chen-Hu was also, in part, supported by the Villum Investigator Grant "WATER" from the Velux Foundation, Denmark.

References

[1] A. Masaracchia, V. Sharma, B. Canberk, O. A. Dobre, and T. Q. Duong, "Digital twin for 6G: Taxonomy, research challenges, and the road ahead," *IEEE Open J. Commun. Soc.*, vol. 3, pp. 2137–2150, Nov, 2022.

[2] M. Hua, Q. Wu, W. Chen, and A. Jamalipour, "Integrated sensing and communication: Joint pilot and transmission design," arXiv:2211.12891 [cs.IT], Nov. 2022.

[3] W. Shen, L. Dai, S. Han, I. Chih-Lin, and R. W. Heath, "Channel estimation for orthogonal time frequency space (OTFS) massive MIMO," in *ICC 2019*, May 2019, pp. 1–6.

[4] H. B. Mishra, P. Singh, A. K. Prasad, and R. Budhiraja, "OTFS channel estimation and data detection designs with superimposed pilots," *IEEE Trans. Wirel.*, vol. 21, no. 4, pp. 2258–2274, Apr. 2022.

[5] Y. Wu, C. Han, and Z. Chen, "DFT-spread orthogonal time frequency space system with superimposed pilots for terahertz integrated sensing and communication," *IEEE Trans. Wirel.*, pp. 1–1, Early Access 2023.

[6] P. Raviteja, K. T. Phan, and Y. Hong, "Embedded pilot-aided channel estimation for OTFS in delay–doppler channels," *IEEE Trans. on Veh. Technol.*, vol. 68, no. 5, pp. 4906–4917, 2019.

[7] Y. Hong, T. Thaj, and E. Viterbo, *Delay-Doppler Communications: Principles and applications*. Elsevier, 2022.

[8] O. A. Aghda, M. J. Omidi, and H. Saeedi-Sourck, "Superimposed channel estimation in OTFS modulation using compressive sensing," arXiv:2212.09280 [cs.IT], Dec. 2022.

[9] H. B. Mishra, P. Singh, A. K. Prasad, and R. Budhiraja, "Iterative channel estimation and data detection in OTFS using superimposed pilots," in *ICC 2021*, 2021, pp. 1–6.

[10] L. Méndez-Monsanto Suárez, K. Chen-Hu, M. J. Fernández-Getino García, and A. García Armada, "Deep learning-aided robust integrated sensing and communications with OTFS and superimposed training," in *IEEE Meditcom 2023*, 2023.

[11] B. Li and W. Yuan, "OTFS communications-assisted environment sensing," in *IEEE JC&S 2023*, 2023, pp. 1–6.

[12] J. E. Volder, "The CORDIC trigonometric computing technique," *IEEE Trans. Comput.*, vol. EC-8, no. 3, pp. 330–334, 1959.